Energies and radiative and nonradiative decay rates of doubly excited $3lnl'$ and $4lnl'$ $(n \geq 4)$ states in Ne^{8+}

H. Merabet,* G. Cremer, F. Frémont, and J.-Y. Chesnel
Laboratoire de Spectroscopie Atomique, Institut des Sciences de la Matière et du Rayonnement, 6, Boulevard du Maréchal Juin, F-14050 Caen Cédex, France

N. Stolterfoht
Hahn-Meitner Institut, Bereich Festkörperphysik, Glienickerstrasse 100, D-14109 Berlin, Germany
(Received 8 May 1995; revised manuscript received 21 February 1996)

Using the multiconfiguration Hartree-Fock code by Cowan, Auger transition energies and radiative and nonradiative decay rates were calculated for doubly excited $3lnl'$ and $4lnl'$ $(n \geq 4)$ states in Ne^{8+}. The results are compared with previous theoretical results. The Auger yields for a given n are averaged over individual states. It is found that the average Auger yields for the configurations $3lnl'$ $(n=4-9)$ decrease slowly with increasing n while they are close to unity for the configurations $4lnl'$ $(n=4-7)$. [S1050-2947(96)03607-4]

PACS number(s): 32.70.Cs, 32.80.Hd

INTRODUCTION

Double-electron capture is one of the most important processes in ion-atom collisions at low energies [1]. Such a process gives rise to doubly excited states which have been studied using the methods of translational spectroscopy [2,3], photon spectroscopy [4–6], and Auger-electron spectroscopy [7–9]. Doubly excited states either autoionize or decay radiatively. Therefore, for the method of Auger spectroscopy, we have to take into account the competing decay when determining absolute cross sections for double-electron capture.

Generally, the Auger decay is dominant when the configurations of equivalent or quasiequivalent electrons $nln'l'$ $(n \approx n')$ are populated during the collision. However, several studies have shown that radiative decay may be important for the configurations of nonequivalent electrons. For example, this is the case for the configurations $2lnl'$ in C^{4+} where the contribution of the radiative decay branch is found to be as large as 80% for $n=7$ [9].

Recently the collision system $Ne^{10+}+He$ has been studied by means of Auger spectroscopy [10–12]. In this system, double-electron capture populates the configurations $4lnl'$ and $3lnl'$ $(n \geq 4)$. The configurations $3lnl'$ and $4l4l'$ decay to the $2l\varepsilon l'$ continuum while the states $4lnl'$ $(n \neq 4)$ autoionize towards the nearest $n=3$ limits. The analysis of the collision system $Ne^{10+}+He$ needs information about atomic structure aspects that manifests itself in Auger line energies and transition rates.

Although a great deal of theoretical work [13–20] has been devoted to doubly excited states in highly-charged ions, no complete study of the atomic aspects has been made for the ion Ne^{8+}. Sánchez and Bachau [19] have determined the energies and partial widths for the states associated with the configurations $4l4l'$. On the other hand, Van der Hart *et al.* [20] have calculated the energies and partial widths for the $4l4l'$ and $4l5l'$ configurations and have also estimated the fluorescence yields for these states. In both cases, the calculations have been performed for a limited number of states. In our work, we provide calculations of Auger transition energies and radiative and nonradiative decay rates for the totality of doubly excited states in Ne^{8+} [i.e., the states associated with the configurations $3lnl'$ $(n=4-9)$ and $4ln'l'$ $(n'=4-7)$], using the Hartree-Fock (HF) code by Cowan [21]. After this work was finished, Van der Hart *et al.* [30] calculated the Auger yields for the configurations $3lnl'$ $(n=7-9)$.

The aim of the present work is the estimate of average L and M Auger yields for the determination of double-capture cross sections in collisions of Ne^{10+} on He. Such theoretical data provide important information for the comprehension of mechanisms giving rise to the double-electron capture [10] as well as to radiative stabilization [11].

AUGER TRANSITION ENERGIES

The energy balance for an Auger transition in the conservative Ne^{8+} system can be written as

$$E_i(Ne^{*8+}) = \varepsilon_a + E_f(Ne^{9+}), \tag{1}$$

where $E_i(Ne^{*8+})$ and $E_f(Ne^{9+})$ are total energies of the multielectron state before and after ionization, respectively, and ε_a is the Auger transition energy. Hence ε_a is determined by calculating separately the total energy of the initial and the final states.

The total energies are determined in two steps. First, zero-order energies of a multielectron system (i.e., two electrons $nln'l'$) are determined by a self-consistent-field (SCF) method that is based on the variational principle. Then, total energies are obtained by diagonalizing the Hamiltonian. The off-diagonal matrix elements include electron-electron interaction as well as spin-orbit interaction [22]. Hence, the en-

*Present address: Department of Physics/220, University of Nevada, Reno, NV 89577-0058.

TABLE I. Total energies obtained by HF calculations in comparison with model potential results by Bachau *et al.* [17] (label *B*). The states are ordered according to increasing energy in each *LS* symmetry. The main $3l4l'$ terms of the wave function are shown with their percentage contributions in parentheses. Contributions smaller than 10% are not given.

LS	Main eigenvector components (%)			$-E_{\mathrm{HF}}$ (eV)	$-E_B$ (eV)	ε_a (eV)
$^1S^e$	$3s4s$ (61)	$3p4p$ (34)		227.07	226.35	113.49
	$3s4s$ (26)	$3p4p$ (24)	$3d4d$ (50)	221.93	221.64	118.63
	$3s4s$ (13)	$3p4p$ (39)	$3d4d$ (48)	214.51	215.33	126.05
$^1P^e$	$3p4p$ (76)	$3d4d$ (23)		226.98	226.24	113.57
	$3p4p$ (20)	$3d4d$ (65)		223.06	222.38	117.50
$^1P^o$	$3s4p$ (40)	$3p4s$ (39)	$3p4d$ (11)	228.20	226.24	112.36
	$3s4p$ (12)	$3d4p$ (40)	$3p4d$ (29)	224.77	224.12	115.78
	$3p4s$ (32)	$3p4s$ (32)	$3p4d$ (23)	224.53	224.00	116.03
	$3d4p$ (11)	$3d4f$ (79)		217.85	217.56	122.71
	$3s4p$ (21)	$3d4p$ (20)	$3p4d$ (36)	216.68	216.55	123.88
$^1D^e$	$3d4s$ (25)	$3s4d$ (57)	$3p4f$ (13)	226.17	225.23	114.39
	$3p4p$ (52)	$3p4p$ (52)		225.87	225.10	114.70
	$3d4s$ (10)	$3s4d$ (14)	$3d4d$ (71)	222.58	222.10	117.98
	$3p4p$ (17)	$3d4s$ (18)	$3p4f$ (58)	219.90	219.49	120.66
	$3d4d$ (21)	$3s4d$ (25)	$3p4f$ (28)	217.26	217.45	123.31
$^1D^o$	$3d4p$ (66)	$3p4d$ (33)		225.32	224.47	115.24
	$3d4p$ (30)	$3p4d$ (55)	$3d4f$ (14)	224.44	223.44	116.12
	$3p4d$ (13)	$3d4f$ (85)		221.71	221.04	118.84
$^1F^e$	$3d4d$ (88)	$3p4f$ (11)		224.80	244.04	115.76
	$3d4d$ (11)	$3p4f$ (88)		223.56	222.84	117.00
$^1F^o$	$3d4p$ (42)	$3p4d$ (49)		226.59	225.75	113.97
	$3d4p$ (11)	$3s4f$ (58)	$3d4f$ (30)	223.22	222.51	117.34
	$3d4p$ (41)	$3p4d$ (22)		220.20	220.10	120.36
	$3p4d$ (28)	$3s4f$ (33)	$3d4f$ (32)	217.60	217.64	122.96
$^1G^e$	$3d4d$ (60)	$3p4f$ (39)		222.45	222.02	118.11
	$3d4d$ (40)	$3p4f$ (59)		218.27	218.48	122.29
$^1G^e$	$3d4f$ (89)			223.64	223.03	116.92
$^1H^o$	$3d4f$ (99)			218.09		122.47

ergies for all singlet and triplet states involved in the configurations $3lnl'$ $(n=4-9)$ and $4ln'l'$ $(n'=4-7)$ were calculated within the intermediate coupling scheme. It is noted that only the interactions within the complex are included in the analysis. Indeed, the most important interactions are those between configurations having the same set of values of the quantum number $\{n_i\}$ [21] (i.e., when the configurations belong to the same complex [23]).

In Table I, we show wave-function compositions, total energies, and Auger transition energies for the singlet states associated with the configurations $3l4l'$. The total energies are compared with calculations using the pseudopotential-Feshbach method [17]. The difference between the two sets of results is less than 1 eV except for the first $^1P^o$ level for which the difference is about 2 eV. This discrepancy may be due to the fact that the configuration interactions of $3l4l'$ with $3lnl'$ $(n\geqslant 5)$ and $4l4l'$ were not included because of the limitation of our calculations using the Cowan code. The comparison of total energies for the singlet states $4l5l'$ with those calculated by the *B*-spline method [20] (see Table II) shows differences of less than 1 eV. Such differences are expected from the present calculations using the Cowan code [22]. In exceptional cases, such as when the states are strongly influenced by configuration interaction, the error of the present method may be as large as a few eV. However, in general, the present HF code gives fairly good results in comparison with other more elaborate theoretical methods [17,20].

RADIATIVE AND NONRADIATIVE DECAY RATES

The radiative decay rates were also calculated using the Cowan code. The total radiative rate is obtained by summing the radiative rates for the decay to all the terms associated with the configurations $1snl$, $2lnl'$, and $3lnl'$. The transitions between $3lnl'$ and $3ln'l'$ $(4\leqslant n'<n)$ as well as the transitions between $4lnl'$ and $4ln'l''$ $(4\leqslant n'<n)$ were not taken into account, since their radiative decay rates are found to be negligible. Thus, one can fairly estimate the total radiative rate by summing over all the allowed transitions of the inner electron (i.e., $3l$ for the configuration $3lnl'$). Hence, the radiative decay rates are expected to be rather constant as a function of the principal quantum number n, as the outer Rydberg electron acts as a passive spectator during the radiative transition. This is clearly seen in Fig. 1 where the example of the singlet $3lnl'$ ^1H was taken.

TABLE II. Total energies, Auger rates, radiative rates, and Auger yields for the singlet states associated with the configurations $4l5l'$ in Ne^{8+}. The present results obtained with the HF code by Cowan are compared with *B*-spline method of Van der Hart *et al.* [20] (label VH). The states are ordered according to increasing energy in *LS* symmetry.

LS	$-E_{HF}$ (eV)	$-E_{VH}$ (eV)	A^a_{HF} (10^{12} s^{-1})	A^a_{VH} (10^{12} s^{-1})	A^r_{HF} (10^{12} s^{-1})	A^r_{VH} (10^{12} s^{-1})	a_{HF} (%)	a_{VH} (%)
$^1S^e$	134.27	133.72	87.8	79.8	0.556	0.538	99.4	99.3
	132.05	131.63	500.3	422.9	0.259	0.301	99.9	99.9
	128.78	128.72	788.0	585.0	0.159	0.390	100.0	99.9
	124.23	125.17	21.7	1.62	0.527	0.535	98.0	75.0
$^1P^o$	134.94	134.31	2.58	3.72	0.642	0.639	98.0	85.0
	133.53	132.93	8.48	12.5	0.234	0.478	97.0	96.3
	133.20	132.76	258.7	216.2	0.672	0.636	99.7	99.7
	131.28	130.75	3.54	10.0	0.241	0.436	94.0	95.8
	130.34	130.21	859.2	651.7	0.404	0.407	99.9	99.9
	127.10	127.54	1.54	6.36	0.141	0.275	92.0	95.9
	125.40	126.33	84.8	64.1	0.594	0.554	99.3	99.1
$^1P^e$	134.38	133.78	3.99	5.86	0.821	1.177	83.0	83.1
	132.75	132.16	10.5	11.3	0.226	0.593	98.0	95.0
	130.24	129.73	0.12	0.19	0.248	0.335	33.0	35.0
$^1D^e$	134.15	133.52	10.07	8.04	0.381	0.389	96.0	95.4
	133.87	133.35	92.98	100.3	0.711	0.650	99.2	99.4
	132.25	131.80	231.9	244.5	0.297	0.320	99.9	99.9
	132.11	131.54	70.11	10.6	0.433	0.402	99.4	96.3
	131.50	131.13	376.1	329.0	0.196	0.686	99.9	99.8
	129.75	129.47	339.0	243.0	0.188	0.255	99.9	99.9
	127.81	127.67	105.2	109.8	0.816	0.487	99.2	99.6
	126.04	126.66	133.3	40.3	0.236	0.498	99.8	98.8
$^1D^o$	133.67	133.07	8.46	9.30	0.579	0.569	94.0	94.2
	133.11	132.63	98.0	93.3	0.682	0.663	99.3	99.3
	131.66	131.08	7.95	6.90	0.107	0.412	99.0	94.4
	130.94	130.60	17.4	16.1	0.267	0.337	98.0	97.9
	129.63	129.11	0.332	0.011	0.124	0.222	73.0	5.0
$^1F^o$	134.46	133.85	5.56	6.64	0.626	0.634	90.0	91.3
	133.21	132.60	9.85	5.35	0.195	0.239	98.0	95.7
	132.51	131.95	215.5	139.0	0.210	0.325	99.9	99.8
	132.34	131.88	181.0	55.4	0.333	0.420	99.8	99.2
	131.10	130.78	450.7	350.0	0.225	0.313	99.9	99.9
	130.33	129.78	91.3	77.4	0.092	0.400	99.9	99.5
	128.01	128.02	270.8	249.0	0.431	0.439	99.8	99.8
	126.45	126.89	175.6	40.1	0.213	0.454	99.9	98.9
$^1F^e$	133.79	133.20	5.89	5.56	0.281	0.449	95.4	92.5
	132.91	132.51	12.7	11.1	0.217	0.421	98.3	96.3
	131.97	131.58	32.7	27.7	0.186	0.587	99.4	97.9
	131.49	130.91	0.223	0.036	0.226	0.219	50.0	14.0
	130.60	130.07	9.57	9.17	0.078	0.357	99.2	96.3
$^1G^e$	133.05	132.38	22.34	67.1	0.160	0.520	99.3	99.2
	132.75	132.37	94.50	30.8	0.285	0.439	99.7	98.6
	131.97	131.27	104.7	125.0	0.161	0.176	99.9	99.9
	130.67	130.30	397.2	282.0	0.160	0.217	100.0	99.9
	129.21	129.12	518.7	437.0	0.088	0.381	100.0	99.9
	126.78	127.26	228.4	94.0	0.218	0.381	100.0	99.6
$^1G^o$	132.52	131.92	4.63	4.41	0.247	0.346	94.9	92.7
	132.15	131.71	9.31	9.21	0.198	0.357	97.9	97.4
	131.85	131.27	18.8	18.1	0.186	0.603	99.0	96.8
	130.88	130.37	11.51	12.0	0.114	0.346	99.0	98.1

TABLE II. (*Continued*).

LS	$-E_{\mathrm{HF}}$ (eV)	$-E_{\mathrm{VH}}$ (eV)	A^a_{HF} (10^{12} s^{-1})	A^a_{VH} (10^{12} s^{-1})	A^r_{HF} (10^{12} s^{-1})	A^r_{VH} (10^{12} s^{-1})	a_{HF} (%)	a_{VH} (%)
$^1H^0$	133.19	132.58	23.28	23.1	0.257	0.339	98.9	98.6
	131.16	130.67	171.4	215.0	0.147	0.481	99.9	99.8
	129.16	129.00	849.3	619.0	0.133	0.217	100.0	100.0
	127.07	127.48	283.8	113.0	0.220	0.432	99.9	99.6
$^1H^e$	132.10	131.53	3.14	8.57	0.175	0.159	94.7	98.2
	131.65	131.09	21.39	0.373	0.072	0.261	99.7	58.8
$^1I^e$	130.85	130.48	942.0	921.0	0.190	0.202	100.0	100.0
	127.44	127.85	578.9	300.0	0.120	0.255	100.0	99.9
$^1I^o$	131.84	131.30	41.8	45.9	0.124	0.113	99.7	99.8
$^1K^o$	127.47	127.79	707.7	378.0	0.147	0.115	100.0	100.0

The results of radiative decay rates for terms associated with the configurations $4l5l'$ are given in Table II. It is seen that the present radiative rates occur in the range from 0.1×10^{12} s^{-1} to 0.8×10^{12} s^{-1} with only three levels (out of 60) with a rate smaller than 10^{11} s^{-1}. The results are also compared with the calculations obtained by Van der Hart *et al.* [20] (Table II). The relative difference between the two methods is less than 30% for the majority of levels. However, it reaches more than a factor of 2 in a few cases. These significant deviations can be attributed to the limitation of our calculations using the Cowan code when configuration interaction becomes too large.

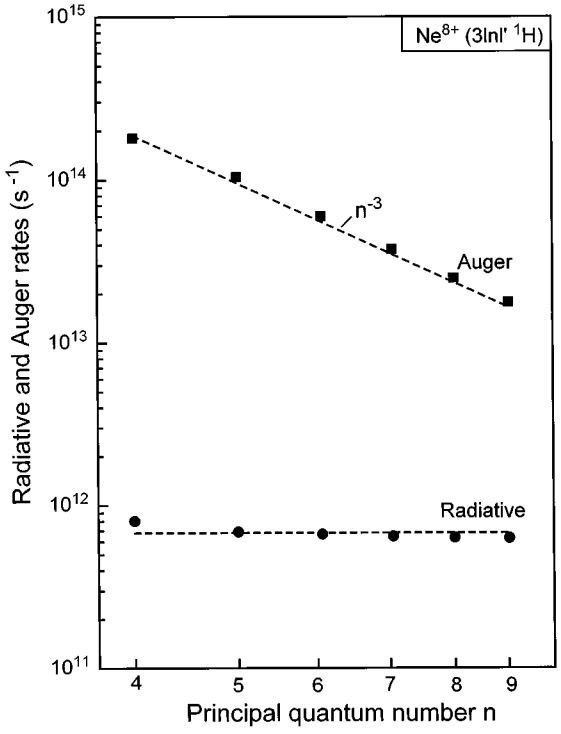

FIG. 1. Radiative rates and Auger rates for the ion Ne^{8+} as a function of the principal quantum number of the outer-shell electron for the fifth ^1H state. The well-known n^{-3} dependence for Auger decay rates is verified while radiative decay rates are rather constant as expected.

The $4l4l'$ states interact strongly with the Rydberg series $3lnl'$ with ($n\geqslant10$). Therefore, we should include the mixing of these configurations when calculating radiative and nonradiative decay rates. Unfortunately, such calculations exceed the abilities of the Cowan code. Thus, we did not take into account for the configuration interaction of the $4l4l'$ states with the Rydberg ones $3lnl'$ ($n\geqslant10$). However, we included the configuration mixing belonging to each complex {4,4}.

Next we focus our attention on the nonradiative decay rates. Calculations were performed for all partial autoionizing widths $A^a_{(3lnl)}$ and $A^a_{(4lnl)}$ involving the final states ($2l\varepsilon l'$ or $3l\varepsilon l'$). The corresponding transition rates are then determined by summing over all the final continuum states.

Auger decay rates for the singlet states $4l5l'$ are compared with calculations performed by the B-splines based method [20]. From Table II, we can see that for most of the levels (43 out of 60), the difference between the Auger transition rates of the two methods is less than 30%. The latter figure can be much larger for a few levels strongly influenced by configuration interaction, as mentioned above. On the other hand, the energy separation of levels is reflected in the wave-function compositions, and the change of these compositions has a considerable influence on the autoionization rates. Therefore, for levels with small Auger rates, the rates could be enhanced dramatically [24]. Finally, it is noted that the wave functions of the Rydberg states $3lnl'$ that depend on the principal quantum number $n^{-3/2}$ are essentially hydrogenic. Hence, the Auger transition rate varies with n^{-3}, as shown in Fig. 1.

AUGER YIELDS

The Auger yield is defined for a given state γ [25] as

$$a_i=\frac{A^a_i}{A^a_i+A^r_i}=\frac{\Sigma_f A^a_{if}}{\Sigma_f A^a_{if}+\Sigma_{f'}A^r_{if'}}, \tag{2}$$

with A^a_{if} and $A^r_{if'}$ the partial autoionization rate and partial radiative rate, respectively. The corresponding total rates A^a_i and A^r_i are obtained by summing over all the allowed transitions.

A comparison of the individual Auger yields with the results given by Van der Hart *et al.* [20] shows good overall agreement (see Table II). The differences between corresponding Auger yields are as small as a few percent. However, large differences are found for the highest $^1D^0$ and the fourth $^1F^e$ level. These disagreements are due to the differences between the Auger rates calculated by the two sets of methods.

The L and M Auger yields $a_L(3ln'l'\gamma J_\gamma)$ and $a_M(4ln'l'\gamma J_\gamma)$ for individual states γ were used to obtain average Auger yields for a given quantum number n' by means of the expression

$$a_{L,M}(n')=\sum_{l,l',J,\gamma}\mathcal{Q}_{n'}(l,l',\gamma,J_\gamma)a_{L,M}(nln'l'\gamma J_\gamma), \quad (3)$$

where $\mathcal{Q}_{n'}(l,l',\gamma,J_\gamma)$, with the normalization $\Sigma_{l,l',\gamma}\mathcal{Q}_{n'}(l,l',\gamma,J_\gamma)=1$, is the probability for the production of the singlet state $|nln'l'\gamma J_\gamma\rangle$ for given n and n'. A simple model was adopted in which this probability is factorized [10],

$$\mathcal{Q}_{n'}(l,l',\gamma,J_\gamma)=q_n(l)q_{n'}(l')p(J_\gamma)s(\gamma), \quad (4)$$

where $q_n(l)$, $q_{n'}(l')$, and $p(J_\gamma)$ are the occupation probabilities associated with the quantum numbers l, l' and J_γ, respectively, and $s(\gamma)$ is the squared coefficient of the singlet component of the intermediate coupling state γ. The probability $p(J_\gamma)$ was set to be proportional to $2J_\gamma+1$. The probabilities $q_n(l)$ and $q_{n'}(l')$ were initially estimated using the model by Burgdörfer *et al.* [26] in the case of 150-keV Ne^{10+}+He collisions. Then, various distributions were tested including the uniform occupation of the quantum numbers l and l'. Moreover, in accordance with experimental results of Meyer *et al.* [27], the population of high-angular-momentum states was included in the distribution $q_{n'}(l')$. On the other hand, calculations have been done by considering the variation of the probabilities $q_n(l)$ and $q_{n'}(l')$ with respect to the collision energy in the range from 10 to 250 keV. As a result of our analysis, we found that the average Auger yield is quite insensitive to the distributions $q_n(l)$ and $q_{n'}(l')$. In the collision, only singlet states may be populated. Hence the summation in expression (3) is carried over only singlet states.

The calculations have been previously performed by setting $s(\gamma)=1$ [10]. In the present work, we take into account that a non-negligible deviation from unity occurs for some $s(\gamma)$ in the case of the configurations $3ln'l'$ (see Table III). However, most of the singlet components dominate in the intermediate coupling states. In fact, the change of the Auger yield is less than 10% if we use $s(\gamma)<1$ instead of $s(\gamma)=1$ in the summation.

The results of average L and M Auger yield calculations are shown in Table III. The M Auger yields are found close to unity, as expected for configurations of quasiequivalent electrons. However, although the majority of the individual Auger yields calculated by means of the Cowan code for the configurations $4l4l'$ are close to 1, there are a few states (4 out of 24) for which the individual Auger yields are found to be nearly equal to zero. These small values of the individual Auger yields affect considerably the average value, which deviates from unity. Indeed, a value of 0.71 [28] is obtained in this case, whereas a value of 0.9 is found by Van der Hart *et al.* [29] for the configurations $4l4l'$ without including the configuration interactions with the $3lnl'$ ($n\geqslant 10$) states. Hence, in this case the B-spline method [29] is more accurate than the Hartree-Fock calculations.

TABLE III. Average L and M Auger yields for a given quantum number n' calculated by means of Cowan code. The results obtained by Van der Hart *et al.* [20] with the assumption of statistical population distribution are also given.

Configurations	$\overline{a}(n,n')$	$\overline{a}_{\mathrm{VH}}(n,n')$
$3l4l'$	0.75	
$3l5l'$	0.67	
$3l6l'$	0.60	
$3l7l'$	0.56	0.59[a]
$3l8l'$	0.52	0.48[a]
$3l9l'$	0.47	0.43[a]
$4l4l'$	0.71	0.90[a]
$4l5l'$	0.91	0.94
$4l6l'$	0.79	
$4l7l'$	0.80	

[a]See Ref. [29].

The mean Auger yield $a_L(n',l')$ for a given quantum number n' decreases strongly with increasing angular momentum l' ($l'\geqslant 3$) as shown in Fig. 2. This is due to the fact that a Rydberg electron with high angular momentum l'

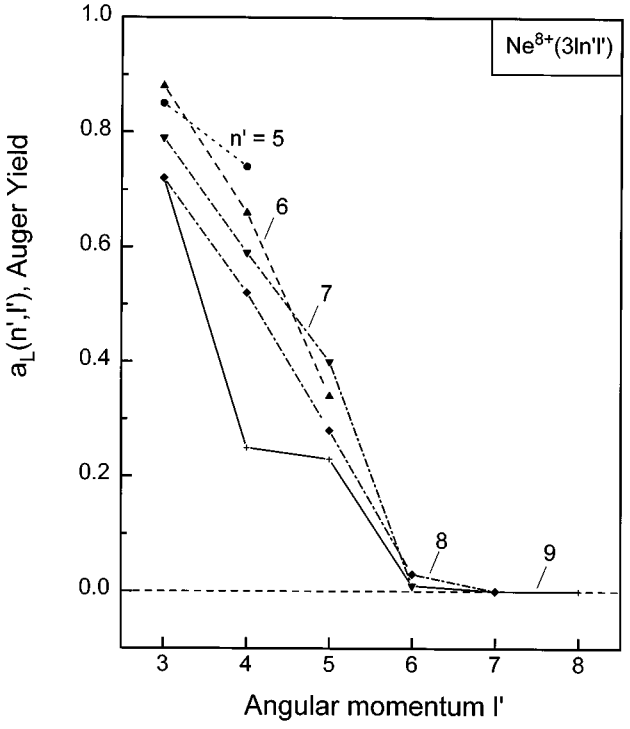

FIG. 2. Mean Auger yield $a_L(n',l')$ for a given quantum number n' as a function of the angular momentum l'. It is seen that $a_L(n',l')$ decreases strongly with increasing angular momentum l' ($l'\geqslant 3$).

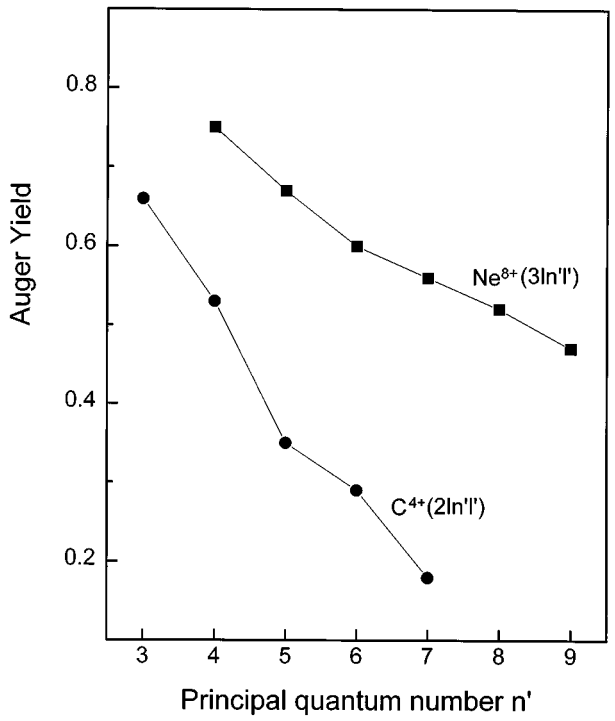

FIG. 3. Mean Auger yields $a_L(n')$ and $a_K(n')$ as a function of the principal quantum number of the outer-shell electron n' for the Ne^{8+} and C^{4+}, respectively. The data of the C^{4+} are from Ref. [9].

moves on a large circular orbit which interacts little with a $3l$ core electron. The L Auger yields decrease relatively slowly with increasing n' in comparison to the K Auger yields for the C^{4+} ion [9] (Fig. 3). This can be understood from the fact that in C^{4+}, besides the transitions from $n=3$ to $1s$, there are transitions from $n=2$ to $1s$ that are relatively important because of the significant radial dipole integral $\langle 1s|r|2l\rangle$. Thus, the radiative rates will decrease when going from C^{4+} to Ne^{8+}. Moreover, the Auger decay rates from $n=3$ to $n=2$ are more important than those of the $n=2$ to $n=1$. Hence, the resulting Auger yields show a relatively small decrease with increasing n' of the outer electron.

CONCLUSION

By using the well-known Cowan code, Auger transition energies and radiative and nonradiative decay rates for the singlet and triplet states for the $3lnl'$ and $4lnl'$ ($n\geqslant 4$) complexes in Ne^{8+} have been determined. Good agreement was found with other more elaborate theoretical methods performed for some of these states. Furthermore, due to the large number of states associated with the populated configurations, and to the width of the experimentally observed peaks, it is not possible to resolve each individual transition in electron spectroscopy experiments. Thus, the knowledge of the Auger energies within the uncertainties given by the Hartree-Fock calculations is sufficient to identify the detected group of peaks [10].

The main goal of this study was calculations of L and M Auger yields. With increasing n', the calculated Auger yields decrease for the configurations $3ln'l'$, and are constant for the configurations $4ln'l'$. The results of our method are mostly close to those given by Van der Hart *et al.* [20] with the assumption of statistical population distribution. It is found that the average values are not dependent on the probabilities $q_n(l)$ and $q_{n'}(l')$ so one may conclude that their choice is uncritical. Finally, the results show that the radiative decay is of minor importance for $4ln'l'$ states, whereas it is considerable for the Rydberg states due to the $3ln'l'$ configurations.

ACKNOWLEDGMENTS

We gratefully acknowledge H. Van der Hart, N. Vaeck, J. E. Hansen, and H. Bachau for providing us with their results prior to publication and for stimulating discussions.

[1] D. H. Crandall, R. E. Olson, E. J. Shipsey, and J. C. Browne, Phys. Rev. Lett. **36**, 858 (1976).
[2] K. Okumo, H. Tawara, T. Iwai, Y. Kaneto, M. Kimura, N. Kobayashi, A. Matsumoto, and S. Turubushi, Phys. Rev. A **28**, 127 (1983).
[3] L. R. Andersson, J. O. P. Pedersen, A. Barány, J. P. Bangsgaard, and P. Hvelplund, J. Phys. B **22**, 1603 (1989).
[4] S. Bliman, J. J. Bonnet, D. Hitz, T. Ludcec, M. Druetta, and M. Mayo, Nucl. Instrum. Methods Phys. Res. Sect. B **27**, 579 (1987).
[5] D. Vernhet, A. Chetioui, J. P. Rozet, C. Stephan, K. Wohrer, A. Touati, M. F. Politis, P. Bouisset, D. Hitz, and S. Dousson, J. Phys. B **22**, 1603 (1989).
[6] P. Boduch, M. Chantepie, D. Hennecart, X. Husson, K. Kukal, D. Lecler, and I. Lesteven-Vaisse, J. Phys. B **22**, L377 (1989).
[7] A. Bordenave-Montesquieu, P. Benoît-Cattin, A. Gleizes, S. Dousson, and D. Hitz, J. Phys. B **18**, L195 (1985).
[8] N. Stolterfoht, C. C. Havener, R. A. Phaneuf, J. K. Swenson, S. M. Shafroth, and F. W. Meyer, Phys. Rev. Lett. **57**, 74 (1986).
[9] N. Stolterfoht, K. Sommer, J. K. Swenson, C. C. Havener, and F. W. Meyer, Phys. Rev. A **42**, 5396 (1990).
[10] F. Frémont, H. Merabet, J.-Y. Chesnel, X. Husson, A. Lepoutre, D. Lecler, G. Rieger, and N. Stolterfoht, Phys. Rev. A **50**, 3117 (1994).
[11] H. Merabet, F. Frémont, J.-Y. Chesnel, G. Cremer, X. Husson, A. Lepoutre, D. Lecler, G. Rieger, and N. Stolterfoht, Nucl. Instrum. Methods Phys. Res. Sect. B **99**, 75 (1995).
[12] A. Bordenave-Montesquieu, P. Moretto-Capelle, A. Gonzalez, M. Benhenni, H. Bachau, and I. Sánchez, J. Phys. B **27**, 4243 (1994).
[13] Y. K. Ho, J. Phys. B **12**, 387 (1979).
[14] A. Macías, F. Martín, A. Riera, and M. Yánez, Phys. Rev. A **36**, 4187 (1987).
[15] Z. Chen and C. D. Lin, J. Phys. B **22**, 2875 (1989).
[16] A. Chetioui, F. Martín, M. F. Politis, J. P. Rozet, A. Touati, L. Blumenfeld, D. Vernhet, K. Wohrer, C. Stephan, M. Barat, M. N. Gaboriaud, H. Laurent, and P. Roncin, J. Phys. B **23**, 3659 (1990).

[17] H. Bachau, F. Martín, A. Riera, and M. Yánez, At. Data Nucl. Data Tables **48**, 167 (1991).
[18] N. Vaeck and J. E. Hansen, J. Phys. B **25**, 3267 (1992).
[19] I. Sánchez and H. Bachau, J. Phys. B **28**, 795 (1995).
[20] H. Van der Hart, N. Vaeck, and J. E. Hansen, J. Phys. B **28**, 5207 (1995).
[21] R. D. Cowan, *The Theory of Atomic Structure and Spectra* (University of California Press, Berkeley, 1981).
[22] N. Stolterfoht, Phys. Rep. **146**, 315 (1987).
[23] A complex is the set of all configurations of given parity that can be formed with a given set of N values of the principal quantum numbers $\{n_i\}$; see D. Layzer, Ann. Phys. **8**, 271 (1959). As an example, in the case of Ne^{8+} (i.e., two electrons) $3s4s+3s4d+3p4p+3p4f+3d4s+3d4d$ forms the even-parity complex $\{3,4\}$.
[24] H. Van der Hart and J. E. Hansen, J. Phys. B **26**, 3297 (1993).
[25] We write the two-electron state $|nln'l'\gamma J_\gamma\rangle$, where J_γ is the total angular momentum and γ labels the states obtained within the framework of the intermediate coupling scheme.
[26] J. Burgdörfer, R. Morgenstern, and A. Niehaus, Nucl. Instrum. Methods B **23**, 120 (1987).
[27] F. W. Meyer, D. C. Griffin, C. C. Hanever, M. S. Huq, R. A. Phaneuf, J. K. Swenson, and N. Stolterfoht, Phys. Rev. Lett. **60**, 1821 (1988).
[28] This value is accidentally the same as the average Auger yields calculated by Van der Hart *et al.* [20] for the $4l4l'$ states with the interaction with the Rydberg series taken into account. H. Van der Hart and J. E. Hansen (private communication).
[29] H. Van der Hart, N. Vaeck, and J. E. Hansen (private communication).